

Interaction Between Fast H_n^+ Clusters and Carbon Foils

N.V. de Castro Faria, Ginette Jalbert and L.F.S. Coelho

*Instituto de Física, Universidade Federal do Rio de Janeiro
Cx.P. 68528, Rio de Janeiro, RJ, 21945-970, Brazil*

Bernadette Farizon-Mazuy, M. Farizon, M.J. Gaillard and S. Ouaskit

*Institute de Physique Nucléaire, Université Claude Bernard-Lyon I
69622, Villeurbanne Cedex, France*

A. Clouvas

Department of Electrical Engineering, University of Thessaloniki GR-54006, Thessaloniki, Greece

A. Katsanos

Technical University of Crete, GR-73101, Chania, Greece

Received November 13, 1995

This work summarizes recent experimental and theoretical results for the interaction of fast H_n^+ clusters with thin carbon foils. The clusters velocities are of the order of the Bohr velocity v_0 and their size numbers n are greater than 3, assuming only odd values. The two topics reviewed are hydrogen atom formation and emission of secondary electrons and, in order to interpret these phenomena, structure calculations are also described.

I. Introduction

“The phenomenon of the scattering and stopping of high speed atomic particles in passing through matter and the accompanying ionization and radiation effects have, as is well known, been one of the most important sources of information regarding the constitution of atoms. Ever since the pioneering work of Thomson and Rutherford, the analysis of the penetration phenomena has been in continual progress and has, in particular, offered many important tests of the gradually refined methods of atomic mechanics. In the course of this development, the topic has been much discussed within the group working at the Institute for Theoretical Physics in Copenhagen and, in this connection, commemoration is above all due to the stimulation of E.J. Williams, whose premature death has been so deplorable a loss. Already about ten years ago, plans were laid for a general treatment of the problem by Williams and the writer but, due

to the isolation brought about by the war, these plans had to be abandoned.”

The paragraph above introduced the superb and already classical 1948 Niels Bohr article^[1] “The penetration of atomic particles through matter”, where an overview of atomic collisions in solids was presented, including energy loss, capture and loss of atomic electrons and range-velocity relations. It condensed all the basic knowledge of this field and established important guidelines for future research. Ever since much work has been done, particularly important being a continuous effort by Lindhard and co-workers^[2]. This effort culminated twenty years later in the LSS theory, a general description for the interaction of atomic projectiles and solid targets, based on the statistical atomic model.

The first collision experiments involving fast molecular ions and solid targets came in 1971, a few years later.^[3] The singly ionized H_2^+ ions were then cho-

sen due to their intrinsic importance as the simplest molecular specie and also due to their easy production in radio-frequency ion sources, commonly employed in Van de Graaff and in multiplier-circuit-type accelerators.

Since the work of Beghian et al^[4], in 1958, it is well known that a beam of fast H_2^+ going through a gas may give, by dissociation, an appreciable amount of hydrogen atoms. The same idea was tested in solid targets where, depending on the ion velocity, the molecule can survive inside the solid and could produce a hydrogen atom in a single collision. The validity of this hypothesis, proposed by Cross^[5] for single protons, was observed as an overproduction of hydrogen atoms in experiments employing H , H_2^+ and H_3^+ beams^[6], and also in several other experiments for the transmission of one- and two- electron projectiles^[7-10]. Some of these experiments used H_3^+ projectiles. These ions, discovered in 1912 by Thomson^[11], present a simple structure, although not so much as H_2^+ , and are also easily extracted from radio-frequency ion sources.^[12]

When H_2^+ or H_3^+ beams incide upon a thin solid target, the respective emerging H_2^+ or H_3^+ ions may not only belong to the transmitted fractions of the original beams but they may also be reconstituted molecules. This reconstitution was observed^[13] for H_2^+ but not for H_3^+ and, in a first stage, the projectile loses its electron on the first layers of the solid and the two protons fly apart (Coulomb explosion). The second stage of the reconstitution occurs if near the exit surface of the target the two protons are not too far one from the other, thus allowing the capture of one target electron in a bound molecular orbital of H_2^+ . Related to this reconstitution process of H_2^+ ions there are two interesting processes, the H atom production enhancement^[14-16] and the H^- ions inhibition.^[16,17]

Recent advances in experimental techniques^[18,19] led to the production and acceleration of hydrogen clusters H_n^+ . The size number n could be equal or greater than five^[19] and presented only odd values^[20],

as predicted by theoretical models^[21-23]. The structure of these clusters has generally been described as H_2 molecules surrounding a H_3^+ ionic core, i.e., $H_3^+(H_2)_m$, where $m=1,2,\dots,n$. In brief, the molecular beam containing clusters of hydrogen is formed by expanding hydrogen gas at certain stagnation conditions of pressure and temperature through a nozzle system, and the electron impact ionization of this hydrogen system produces cluster ions. The charged clusters may be accelerated and mass analysed^[25] or, less commonly, trapped in a radio-frequency octupole ion guide.^[26]

The interaction of these clusters with thin amorphous carbon foils ($\sim 100 \text{ \AA}$) was recently studied for energies in the 10 to 700keV/u range.^[27-30] Transmission of these clusters through an amorphous film as well as their reconstitution are very improbable events and were never observed. However, the formation of H in the ground^[26] and excited^[27,29] states and the emission of secondary electrons,^[30] both induced by these fast H_n^+ clusters, are important sources of knowledge of these cluster-solid interactions.

As an introduction to the main topics, this work initially analyses the charge exchange processes between protons or atomic hydrogens and amorphous films and describes results concerning the simplest hydrogen "cluster", H_2^+ . Afterwards, it presents calculations of the H_n^+ structure with *ab initio* methods. Finally, the experimental and theoretical aspects of these two phenomena - charge exchange and emission of secondary electrons - are discussed for larger clusters.

2. Transmission of fast light ions through solids

At least two kinds of experiments indicate that one or two electrons can stay correlated with fast protons or alpha particles inside a solid film. The first is the transmission, for example, of H, He^+ and He through carbon foils (Fig. 1). Plotted against the dwell time τ , a characteristic feature of the transmission is an exponential decay for small τ values^[7], levelling off to a

constant value corresponding to the respective equilibrium charge fraction. The second is the velocity dependence of the transmitted fraction^[9] of He⁺. In that experiment it was shown that, for the range of velocities considered, the n=1 and n=2 states could survive inside the target but not the n=4 state. It was also possible to observe the approximated velocity threshold for the existence of the 3p state (Fig. 2).

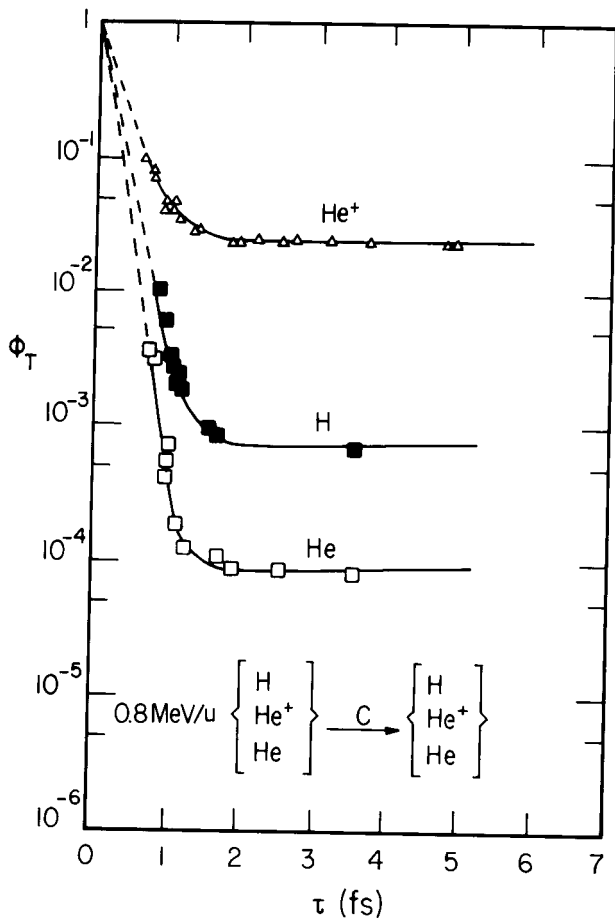


Figure 1. Transmitted fraction Φ_T of incident 0.8 MeV/u H, He⁺ and He through carbon foils as a function of τ , the projectile dwell time in the target. The curves show the least square fitting of the data by the function $\Phi_T = (1 - \Phi_{i\infty})exp(-\tau/\tau_i) + \Phi_{i\infty}$ (ref.7), where $\Phi_{i\infty}$ are the equilibrium charge fractions and τ_i the projectile mean lifetime.

The main argument against the existence of a stationary state of fast projectiles is the dynamic screening of the moving charge by the target electrons. A simple analytic approximation formula for nonrelativistic hydrogenic energy levels in the presence of this screening has been recently obtained, from classical scaling invariances, by Müller and Burgdörfer^[31], where the elec-

tron gas was described by a dielectric function $\epsilon(k, \omega)$ in the plasmon-pole approximation. They got for n=3 a threshold of $v=3.6a.u.$, identical to the experimental value, although one may argue about the possibility of calculating and measuring sharp thresholds. The calculation of the threshold by the extrapolation of energy level shifted to the ionization limit ($E=0$) is not simple because near the ionization limit it is impossible to identify each energy level. Otherwise, the collisional broadening of these levels is expected to smear out any sharp threshold. In that context, the perfect coincidence between experimental and theoretical values seems to be partially fortuitous, but it nevertheless demonstrates the existence of a transition region.

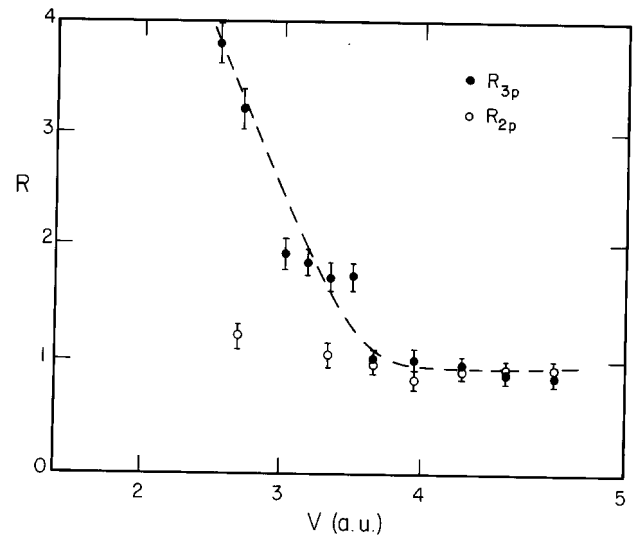


Figure 2. Velocity dependences of R_{3p} and R_{2p} , normalized to unity for $v = 3.7$ a.u., where $R_{np} = F_1(np)/F_1$ and F_1 is the He⁺ fraction in the emerging beam (Ref. 9).

The passage of the molecular ion H₂⁺ through thin carbon foils is illustrated in Fig. 3 (Ref. [13]). Similarly to the atomic case, the ions being transmitted with their original electrons are identified by an exponential attenuation curve that goes to unity when τ goes to zero. However, the reconstituted particles lead to a departure from this dependence, more visible at large τ values. The major difference from the atomic case is the absence of H₂⁺ equilibrium yields for thick targets. This is due to the Coulomb explosion, as the distance between the two H₂⁺ protons grows with the dwell time

and, consequently, the probability of H_2^+ reconstitution falls as τ increases.

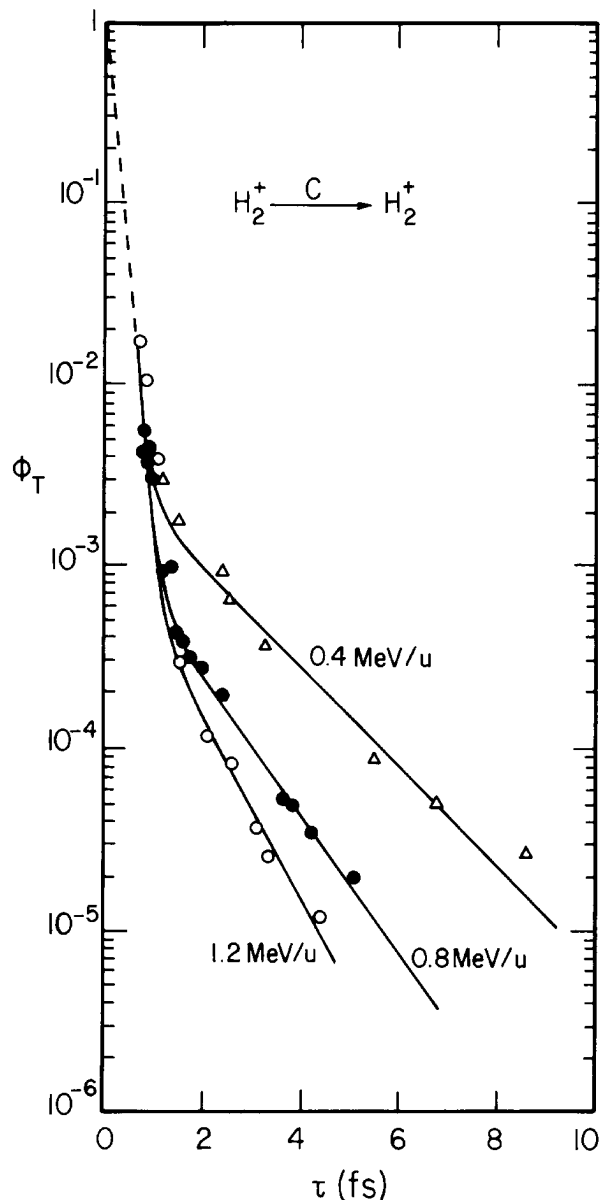


Figure 3. Transmitted fraction Φ_T of incident 0.4, 0.8, and 1.2 MeV/u H_2^+ through carbon foils as a function of τ , the projectile dwell time in the target. The curves were drawn only to guide the eye (Ref. 8).

Fast H_2^+ ions incident upon carbon foils can also produce H and H^- atoms. Fig. 4a shows the ratios of the H yields produced by H_2^+ to the corresponding ones for H^+ projectiles, plotted as function of the dwell time.^[16,17] Fig. 4b shows the τ dependence of the H^- fraction. For small dwell times the presence of the incident electron of H_2^+ in the H and H^- leads to ratios and fractions larger than their equilibrium values, reached

for large dwell times. For intermediate τ values the H ratio presents values larger than unity, the reverse being true in the H^- case. These enhancement and inhibition effects for intermediate dwell times were confirmed using D_2^+ projectiles at the same velocities. These two phenomena have different origins.

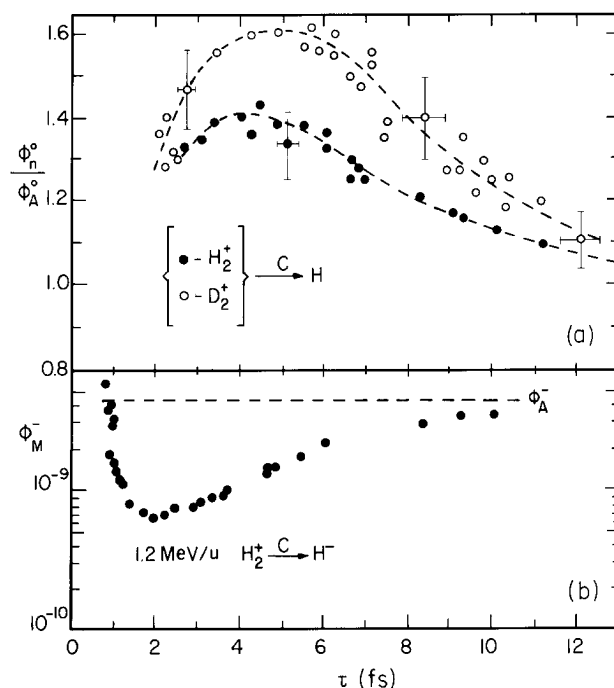


Figure 4. Experimental values for H^- and H production. (a) Ratio of the atomic hydrogen fractions produced by molecular (H_2^+ and D_2^+) and by atomic projectiles after traversal of carbon foils, given as function of the dwell time τ . The broken curves were drawn only to guide the eye. (b) H^- fraction produced after traversal of carbon foils by 1.2 MeV/u H_2^+ , given as function of the dwell time τ . The broken horizontal line represents the equivalent H^- equilibrium fraction obtained with atomic projectiles (Ref. 16).

The inhibition in the H^- production is a post-foil effect. First the diproton makes a double electron capture in the last layers of the solid into a molecular orbital asymptotically correlated with a negative hydrogen ion plus a proton. After capturing the two electrons and surviving the H_2 formation, the diproton moves outside the foil as dictated by the Coulomb explosion. In the center-of-mass of the system the H^-+H^+ pair is the receding stage of a zero-impact parameter collision (a “half-collision”) and neutralization, i.e. a process leading asymptotically to a pair of hydrogen atoms, can then occur. This collision, when described in the

Landau-Zener approximation, reproduces remarkably well the experimental data.

The enhancement of the H production is essentially due to the processes of electron capture and loss by the diproton system still inside the foil. From the point of view of the dynamical screening of one proton, i.e., the lowering of the binding energy, the electron capture is less influenced than the electron loss, because the projectile captures almost localized electrons (conservation of momentum and energy) near carbon nuclei. Consequently, the delocalized electrons play a small role in the capture by one proton but are essential in the electron loss due to their dynamical screening. Otherwise, as will be further discussed in section 4, in the H_2^+ case the electron capture is also not affected by “vicinity” effects but the electron loss is reduced due to the increase of the electron binding energy.

One limitation of the theoretical analysis of experiments with accelerated H_2^+ and H_3^+ ions is presented by the internal energy, both vibrational and rotational, of the molecular ions produced in the currently employed radio-frequency ion sources. This results in very broad distributions of the internuclear distances. A source with larger residence time for the ions was pointed to be the solution and a storage ion source based on the principle of confinement of charged particles by inhomogeneous electric fields was able to produce H_2^+ ions in low vibrational states.^[32] Feeding the ion source with a gas mixture of H_2 and noble gases (He and Ne) at high pressures, the excited vibrational states of H_2^+ ions were effectively quenched by ion-molecule reactions and collisional deactivation. With a 1:5 ratio and a H_2 +Ne mixture the H_2^+ ions were found to be predominantly in the $\nu=0$ and $\nu=1$ states. H_3^+ is formed in a plasma via the reaction $H_2^+ + H_2 \rightarrow H_3^+ + H$, with an initial internal energy of about 2 eV. When the radio-frequency trap ion source operating with the same mixture - H_2 +Ne at 1:5 ratio - is employed, the internal energy of the H_3^+ ions has been measured^[32] to be less than 0.5 eV. These results suggest that the H_3^+ ions formed in the ion

source have relaxed so that only the first and possibly the second vibrational levels remain populated.

3. H_n^+ structure

The term “cluster” is usually used to describe aggregates of atoms that are too large to be considered molecules and too small to resemble an object, even a tiny one. The hydrogen clusters H_n^+ are of the covalent type and, at least for small n values, they can be well described by standard quantum chemistry calculations.^[22–24,34–36] All these studies conclude that an equilateral triangle H_3^+ serves as nucleating agent for H_2 . Moreover, besides H_2^+ , there is an experimentally obtained cluster structure^[37–39] only for H_3^+ .

3.A. Experiment

The technique here described is based on the Coulomb explosion phenomenon. It has been applied for H_3^+ and other light ions but may, in principle, be extended for other H_n^+ clusters. Consider a well collimated H_3^+ beam with energy in the hundred keV range, incident on a thin (~ 100 Å) carbon foil. When the molecular ion enters the solid target its two binding electrons are stripped off. During the target traversal the resulting three protons remain essentially stripped, forming a “crowd” that undergoes an “explosion”, as the initial coulombic potential energy is converted into kinetic energy.

The relatively high cluster velocity has several interesting consequences. First, it minimizes the multiple scattering inside the target. It also results in the fully stripped protons, as electron capture is negligible at these high velocities. Lastly, it provides an amplifying effect for the small molecular potential energy. This effect leads to the possibility of easily measuring the velocity distribution for the emergent protons. These measurements and the angular distribution for spatially correlated pairs of protons are the bases for several methods which study the H_3^+ structure and, to

illustrate this point, we will sketch one of the three methods described in reference 37.

It was assumed that, after the dissociation of 2.2 MeV H_3^+ in a thin carbon foil, the beam was composed by three correlated protons (all other possibilities such as HH_2^+ , HH^+H^+ and H^+H_2^+ were either totally negligible or accountable for from other experiments). This beam incided upon a movable surface barrier detector with a small frontal collimator. The pulse height distribution from the detector had three peaks, corresponding to the approximate energies of one, two and three $\text{E}(\text{H}^+)$, as the time interval among the arrival of two or three correlated protons is smaller than the time resolution of the detector system. The three $\text{E}(\text{H}^+)$ peak presented few events. The accidental coincidences of two protons from distinct molecules were in a small number and could be properly subtracted. The only way an incident molecule has to produce an off-axis proton pair is entering the target with two protons aligned along the beam direction. It is clear that the signature of a colinear configuration is an event in the 3E peak centered at 0° . In fact, due to the possibility of destruction of the triple coincidence by multiple scattering in the target, a 2E central peak would be more probable. From calculations that include Coulomb explosion and multiple scattering, the two protons angular distribution could be reproduced with the proton-proton distance being the free parameter to be determined.

A completely different experiment, also obtaining the proton-proton distance, is described in reference 39. It is based on the knowledge of the three fundamental bands of H_2D^+ and on their relationship to the equilibrium structure of H_3^+ . A high resolution absorption spectrum of the H_2D^+ ion was obtained in the 2010-2610 cm^{-1} region through the employment of two types of tunable monochromatic laser sources. This data, together with two already known microwave absorption lines, was fitted by theoretical models. When the supermatrix model is employed (a model where the Hamiltonian is set up in a large rovibrational basis and

directly diagonalized) we can get the equilibrium rotational constants. From these constants the structural parameters can be derived, in particular the equilibrium bond distance of H_3^+ .

3.B. Theory

Much of our understanding of the structure and collision dynamics of cluster ions has relied on the result of calculations.^[22–24,34–36] Moreover, it is obviously desirable to carry out non-semi-empirical or *ab initio* calculations whenever possible. This is fortunately the case of the H_n^+ covalent bond hydrogen clusters for small n . The stereochemical structure of the clusters being the main interest of our review and not, for example, dipole moments or infrared transition intensities, we will base our presentation in the work of M. Farizon *et al.*,^[22–24] where self consistent field (SCF) Hartree-Fock calculations have been carried out for H_n^+ , $n = 3$ to 13 (odd). Configuration interaction calculations with single plus double substitutions have been included. These calculations were performed with a Gaussian code^[40] where the basis set is the contracted gaussian function.

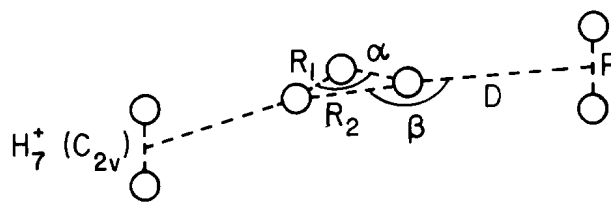


Figure 5. Energy and structure of H_7^+ (ref. 22).

Fig. 5 presents one example of the parameters employed in a particular structure calculation, the H_7^+ cluster with C_{2v} symmetry. The energy and the structure parameters were calculated at several levels of theory: triple zeta plus polarization (TZP) basis set with SCF Hartree-Fock, configuration interaction including single and double excitations (CISD), and fourth-order Moller-Plesset calculations (MP4). The results show a deformation of the H_3^+ core which differs in a significant way from the H_5^+ case, as shown in Fig. 6. Also the distance between H_2 and the nearest proton is 0.21 Å

greater than the corresponding one for the H_3^+ cluster. This length and the value of the β angle ($\sim 148^\circ$) can be related to the repulsion between two H_2 subunits. For this structure, the H_3^+ core subunit is found to be more equilateral at the SCF level than in the CISD calculations.

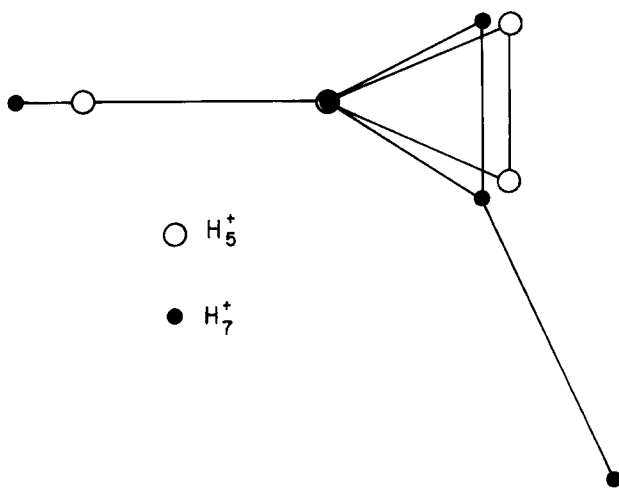


Figure 6. Deformation of the H_3^+ "core" for H_5^+ and H_7^+ , observed in the H_3^+ plane (ref.22).

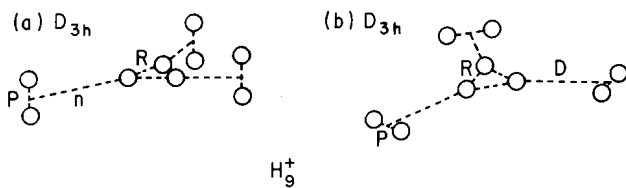


Figure 7. Energy and "shape" of two "in principle" H_9^+ conformers, with the same symmetry (Ref. 22).

Fig. 7 illustrates two possible conformer structures for H_9^+ with the same symmetry D_{3h} , structure (a) clearly describing better the cluster. In fact, calculations with conformer (b) give imaginary frequencies and only (a) exhibits a minimum in the potential energy surface at these levels of theory. Besides being time-consuming, these calculations are therefore of complex interpretation, these two features limiting the structure calculation for very large clusters. Calculations were made, however, till $n=15$ by Farizon *et al.*^[24]

4. Fast H_n^+ incident in carbon foils

4.A. Hydrogen atom formation

Hydrogen cluster beams of energies ranging from 40 to 700 keV are currently delivered by the multiplier-circuit-type accelerator of the Institut de Physique Nucléaire de Lyon (France). The accelerated cluster ion beam is energy- and mass-selected by electrostatic and magnetic analysers. Beams of H_n^+ ($n=2$ and $n=3$ to 61, odd) with energies as high as 630 keV were used in the experiments. The cluster bursts last approximately 60 ms with a repetition rate of ~ 0.2 Hz.

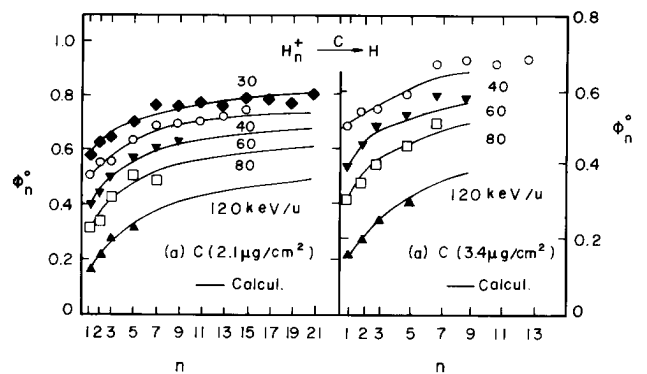


Figure 8. H fraction after the traversal of carbon foils by 30, 40, 60, 80, and 120 keV/u hydrogen clusters H_n^+ as a function of the proton number n . Solid curves are calculations (Ref. 41).

Two kinds of measurements were done. In the first^[26] the cluster beam incides upon a carbon target, all charged fractions were deflected and the total neutral fraction ϕ_n^0 was measured. The main feature of ϕ_n^0 (Fig. 8) is its increase with n , for a given velocity, and then a tendency to saturate for $n \geq 7$. This almost linear increase is in qualitative agreement with previous observations for H_2^+ and H_3^+ projectiles and reflects essentially the fact that the average distance between the protons at the exit surface is quite the same, notwithstanding the cluster mass. In the second,^[28] we determine the fraction of H fragments that are in the $2p$ excited state after exiting the carbon foil. This was

ties, an interpolation was made employing He, N and O values.

If now we have an H_n^+ cluster inciding upon a foil and leading to the production of H atoms, it will be assumed that the already discussed expressions for an isolated proton still hold. This problem may be described as a proton i , surrounded by the "crowd" of $(n - 1)$ protons j , that captures one electron in its $1s$ state. Its ionization energy is equal to the sum of the generalized molecular energy B_{1s} of the n protons inside the solid, assumed equal to I_{1s}^{solid} , with the screened repulsion energy, which depends upon the screening parameter η . Figures 8 and 10 present the results of our calculations, together with our experimental data, and the good agreement seems to indicate that charge exchange, screening and vicinity effects were the bases of the observed phenomena.

4.B. Secondary electron emission

Secondary-electron-emission (SEE) is defined as the emission of electrons by solid targets bombarded with fast particles. In order to describe this effect a useful parameter is the total secondary-electron yield γ , defined as the number of ejected electrons per incoming projectile.

SEE from thin carbon foils bombarded with H_n^+ hydrogen clusters has been recently measured,^[30,44] for projectile velocities around and above the Bohr velocity. Before these measurements it was already known^[45] that the γ values for fast H_2^+ and H_3^+ ions at the same velocity were not proportional to the number of protons in the projectile. Defining a reduced ratio $R_n = \gamma(H_n^+) / n\gamma(H^+)$, when R_n deviates from unity there is an evidence of cluster effects. In fact, it was verified that, in the energy range $10 \text{ keV/u} < E < 1.2 \text{ MeV/u}$, R_n increases with the projectile velocity, going from values smaller to values greater than unity.

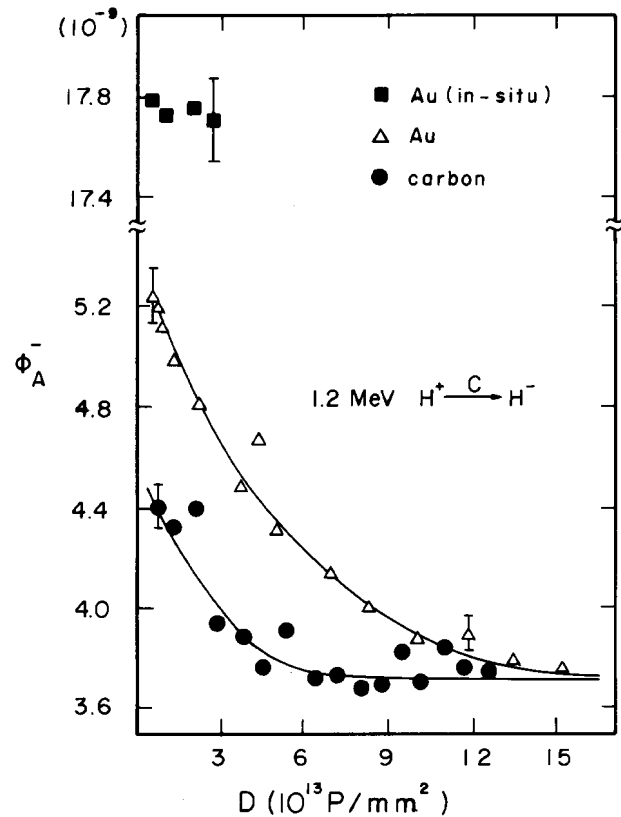


Figure 11. Φ^- equilibrium fraction for protons inciding in carbon, gold and gold evaporated *in situ* targets, versus the irradiation dose in 10^{13} protons/ mm^2 . The data shown in the upper part was obtained with a gold layer freshly evaporated onto the exit target surface, while the lower part shows data for gold and carbon targets prepared before being mounted inside the chamber (Ref. 47).

Electron emission is known^[46] to be very sensitive to the target surface. A very striking demonstration of the importance of the target last layer for a phenomena also occurring at the surface was presented in reference 47. In that work a proton beam incided upon several targets - a "normal" carbon foil, several gold targets prepared outside the bombarding chamber and a gold layer freshly evaporated (*in situ*) - and the production of fast H^- ions was recorded. As H^- ions do not survive inside the solid target due to its small affinity (0.75 eV), any one exiting the foil was formed within the last five atomic layers. In this aspect the H^- formation is a better surface probe than SEE, as the secondary electrons originate mainly from 10-20Å below the solid surface. Fig. 11 shows the equilibrium ratio for (1) a gold layer freshly evaporated onto the exit surface and irradiated with a small proton dose (upper part), (2) a gold tar-

get prepared before being mounted inside the chamber (middle part) and (c) a carbon target evaporated similarly as (2). Two interesting facts may be observed in this figure. For a small dose the gold equilibrium fraction in case (1) is three times as large as in case (2) and for a large dose cases (2) and (3) reach the same value, i.e., the last layers are neither carbon nor gold but impurities deposited on the original target.

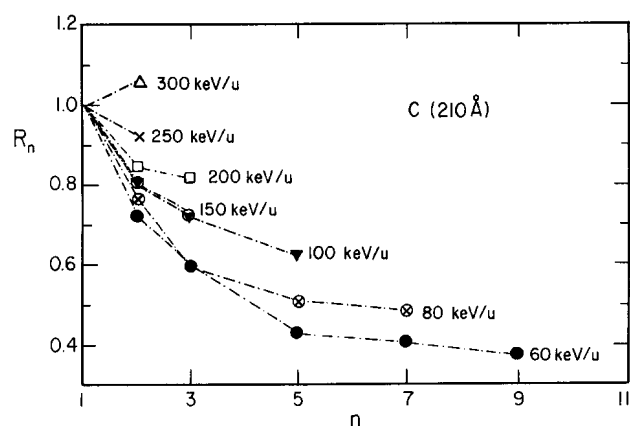


Figure 12. Cluster mass number dependence of $R_n = \gamma(H_n^+)/n\gamma(H^+)$ for projectile velocities in the 60-300 keV/u range and for a 210 Å carbon foil (Ref. 30).

Bearing this fact in mind, Fig. 12 (reference 30) shows R_n as a function of n , the cluster mass number, for several projectile velocities (60-300 keV/u) and for a 210 Å dirty surface carbon foil (10^{-6} Torr). Except for 300 keV/u, the highest velocity, clusters in all the measured range of mass numbers show an inhibition effect with respect to the proton case ($R_n < 1$). From these results R_n equal to unity is reached for incident energies between 250 and 300 keV/u. This agrees with an experimental result^[48] which yielded $R_2=1$ for H_2^+ ions incident on a copper target at 200 keV/u.

Two qualitative comments may be made about the results presented in figure 12. First, for a given velocity and a given target thickness, R_n initially increases with n and then reaches a saturation value for n around 5 or 7. Second, for a given n and a given target thickness, R_n increases with decreasing velocity down to 60 keV/u although, below this point, the results³⁰ seem to present a different velocity dependence.

These strong inhibition effects could appear in backward and forward electron emission and, at the range of velocities being studied, both emissions present the same order-of-magnitude, not only for protons but also for clusters.^[43,46] However, due to the screened Coulomb explosion, the cluster effect is supposed to act differently at the entrance and the exit of the target. In fact, at the entrance the cluster has the same dimensions as in the free space but, depending on the time spent inside the foil, at the foil exit the average distance between protons may be very large and the protons behave as almost independent particles.

Reference 44 shows that, for a target thickness of 950 Å, surprisingly low forward electron yield ratios were obtained, about 0.7 for $n=5$ and 0.9 for $n=2$, even at energies as low as 40 keV/u. As the mean distance between the protons at the exit surface is about 15 Å in some sense, at least in respect to SEE, it seems that these protons keep some correlation over unexpectedly large distances.

Otherwise, for the velocity range considered in these works the dominant electron production mechanism is the kinetic emission, where the initial step is the direct transfer of kinetic energy from the projectiles to the target electrons. A fraction of these electrons moves from the bulk towards the target surfaces and some pass through the surface. Thus, the kinetic emission is related to the fraction of the projectile kinetic energy which is transferred to target electrons, i.e., the electronic energy loss. This statement is demonstrated by the proportionality, within a few percent, found between the electron yields and the stopping power, essentially electronic energy loss, when employing protons as projectiles and for a wide range of energies going from 10 keV to 10 MeV. The question is thus to understand why there are effects that inhibit or enhance the secondary electron emission differently from the electronic energy loss case.

These results could be possibly explained by a more careful analysis of the H_2^+ , the H_3^+ , and the H_n^+ actual

structures. Firstly, as the H_2^+ and the H_3^+ molecular ion beams are mostly in excited ro-vibrational states, the mean distances between protons are larger than the distances calculated for a molecule in its fundamental state. The mean distance is about 1.3 Å for H_2^+ and 1.2 Å for H_3^+ . Concerning H_n^+ clusters, they are weakly bound and no important vibrational excitation either in the H_3^+ core or in the H_2 subunits can take place, with the distance between the H_2 protons being close to the theoretical ground state distance (0.74 Å)^[22,29]. For the velocity range here studied, it was demonstrated^[40] that the dynamic screening length introduced by the electrons of a carbon target varied between 0.7 and 1.0 Å. Therefore, in the first layers of a target, an electron belonging to a cold H_2 molecule in a cluster will stay bound over a distance longer than that for an usual H_2^+ molecular ion, directly produced inside an ion source fed with H_2 gas. This fact could explain not only the correlation over unexpectedly large distances of the protons of the original cluster, but also part of the discrepancy between secondary electron emission and electronic energy loss results.

5. Conclusions

Regarding the two reviewed topics, i.e. hydrogen atom formation and emission of secondary electrons, one important point is the fact that the collective effect is the same for all H_n^+ clusters (one additional H_2 molecule to a H_n^+ cluster does not furnish a supplementary collective effect). This aspect could be better described by comparing the results here presented to experimental data obtained from other clusters, as C_{60} for example, with different geometries possibly giving rise to different effects. Another possible study, which our group intends undertake in the near future, is the incidence of H_n^+ upon other solid targets, such as aluminium, gold, etc, changing in this case the screening distance.

Other topics regarding the interaction of fast clusters of heavy atoms with solids, as energy loss and ma-

terials modifications, are very interesting due to the large density of the energy transferred to the material and have been recently reviewed^[49,50]. Such experiments are, in particular, being performed with 10-50 MeV Au_4 and C_{60} clusters and metallic and organic targets^[51].

Acknowledgements

This work was partially supported by FINEP (Brazil), CNPq (Brazil) and IN₂P₃-CNRS (France).

References

1. N. Bohr, Mat. Fys. Medd. Dan. Vid. Selsk. **18**, no. 8 (1948).
2. J. Lindhard and M. Scharff, Mat. Fys. Medd. Dan. Vid. Selsk **27**, no.15 (1953);
J. Lindhard, Mat. Fys. Medd. Dan. Vid. Selsk **28**, no.8 (1954);
J. Lindhard, M. Scharff and H.E. Schiott, Mat. Fys. Medd. Dan. Vid. Selsk **33**, no. 14 (1963);
J. Lindhard, Vibeke Nielsen, M. Scharff and P.V. Thomsen, Mat. Fys. Medd. Dan. Vid. Selsk **33**, no. 10 (1963);
J. Lindhard, Vibeke Nielsen and M. Scharff, Mat. Fys. Medd. Dan. Vid. Selsk **36**, no. 10 (1968).
3. J.C. Poizat and J. Remillieux, Phys. Lett. **34A**, 53 (1971).
4. L.E. Beghian, R.P. Scharenberg, P.H. Rose and Wanick, Phys. Rev. **110**, 1479 (1958).
5. M.C. Cross, Phys. Rev. B **15**, 602 (1977).
6. M.J. Gaillard, J.C. Poizat, A. Ratkowski, J. Remillieux and M. Auzas, Phys. Rev. A **16**, 2328 (1977).
7. N. Cue, N.V. de Castro Faria, M.J. Gaillard, J.C. Poizat and J. Remillieux, Nucl. Instr. Meth. **170**, 67 (1980).
8. M.J. Gaillard, J.C. Poizat and J. Remillieux, Phys. Rev. Lett. **41**, 159 (1978).
9. M.Chevallier, A. Clouvas, N.V. de Castro Faria, B. Farizon-Mazuy, M.J. Gaillard, J.C. Poizat and J. Remillieux, Phys. Rev. A **41**, 1738 (1990).

10. N. Cue, N.V. de Castro Faria, M.J. Gaillard, J.C. Poizat and J. Remillieux, *Phys. Lett.* **72A**, 104 (1979).
11. J.J. Thomson, *Philos. Mag.* **24**, 209 (1912).
12. J.G. Rutherglen and J.F.I. Cole, *Nature* **160**, 454 (1947).
13. N. Cue, N.V. de Castro Faria, M.J. Gaillard, J.C. Poizat, D.S. Gemmell and I. Plessner, *Phys. Rev. Lett.* **45**, 613 (1980).
14. M.J. Gaillard, J.C. Poizat, A. Ratkowski and J. Remillieux *Nucl. Instr. Meth.* **132**, 69 (1976).
15. A. Clouvas, M.J. Gaillard, A.G. de Pinho, J.C. Poizat, J. Remillieux and J. Desesquelles, *Nucl. Instr. Meth. Phys. Res. B* **2**, 273 (1984).
16. N.V. de Castro Faria, F.L. Freire Jr, E.C. Montenegro and A.G. de Pinho, *J. Phys. B* **19**, 1781 (1986).
17. N. Cue, N.V. de Castro Faria, M.J. Gaillard, J.C. Poizat and J. Remillieux, *Phys. Rev. A* **22**, 388 (1980).
18. W. Henkes, V. Hoffman and F. Mikosch, *Rev. Sci. Instrum.* **48**, 675 (1977).
19. A. Schempp and H.O. Moser, *J. de Phys.* **C-2**, 205 (1989).
20. M. Chevallier, N.V. de Castro de Faria, B. Farizon-Mazuy, M.J. Gaillard, J.C. Poizat and J. Remillieux, *J. de Phys.* **C-2**, 189 (1989).
21. Y. Yamaguchi, J.F. Gaw, R.B. Regmington and H.F. Schaefer III, *J. Chem. Phys.* **86**, 5072 (1987).
22. M. Farizon, B. Farizon-Mazuy, N.V. de Castro Faria and H. Chermette, *Chem. Phys. Letters* **177**, 451 (1991).
23. M. Farizon, H. Chermette and B. Farizon-Mazuy, *J. Chem. Phys.* **96**, 1325 (1992).
24. B. Farizon-Mazuy, M. Farizon, H. Chermette and M.J. Gaillard, to be published.
25. Y. Chanut, J. Martin, R. Salin and H.O. Moser, *Surf. Sci.* **106**, 563 (1981).
26. M. Okumura, L.I. Yehand and Y.T. Lee, *J. Chem. Phys.* **88**, 79 (1988).
27. B. Mazuy, A. Belkacem, M. Chevallier, M.J. Gaillard, J.C. Poizat and J. Remillieux, *Nucl. Instr. Meth. Phys. Res. B* **28**, 497 (1987).
28. M. Farizon, A. Clouvas, N.V. de Castro Faria, B. Farizon-Mazuy, M.J. Gaillard, E. Gerlic, A. Denis, J. Desesquelles and Y. Ouerdane, *Phys. Rev. A* **43**, 121 (1991).
29. M. Farizon, N.V. de Castro Faria, B. Farizon-Mazuy and M.J. Gaillard, *Phys. Rev. A* **45**, 179 (1992).
30. N.V. de Castro Faria, B. Farizon-Mazuy, M. Farizon, M.J. Gaillard, Ginette Jalbert, A. Clouvas, A. Katsanos, and S. Ouaskit, *Phys. Rev. A* **46**, R3594 (1992).
31. J. Müller and J. Burgdörfer, *Phys. Rev. A* **43**, 6027 (1991).
32. A. Sen, J.W. McGowan and J.B.A. Mitchell, *J. Phys. B* **20**, 1509 (1987).
33. A. Sen and J.B.A. Mitchell, *J. Phys. B* **19**, L545 (1986).
34. Y. Yamaguchi, J.F. Gaw and H.F. Schaeffer III, *J. Chem. Phys.* **78**, 4074 (1983).
35. K. Hirav and S. Yamabe, *Chem. Phys.* **80**, 237 (1983).
36. H. Huber, *J. Mol. Struct. (Theochem)* **121**, 287 (1985).
37. M.J. Gaillard, D.S. Gemmell, G. Goldring, I. Levine, W.J. Pietsch, J.C. Poizat, A. Ratkowski, J. Remillieux, Z. Vager and B.J. Zabransky, *Phys. Rev. A* **17**, 1797 (1978).
38. H. Martínez, I. Alvarez, J. de Urquijo, C. Cisneros and A. Amaya-Tapia, *Phys. Rev. A* **36**, 5425 (1987).
39. S.C. Foster, A.R.W. McKellar, I.R. Peterkin, J.K.G. Watson, F.S. Pan, M.W. Crofton, R.S. Altman and T. Oka, *J. Chem. Phys.* **84**, 91 (1986).
40. (a) W.J. Hehre, L. Radon, P.R. Schleyer and J.A. Pople, *Ab initio* molecular orbital theory, Wiley (1986); (b) Quantum Chemistry Program Ex-

- change, QCPE-525, Department of Chemistry, Indiana University, Bloomington, IN (1986).
41. M. Farizon, N.V. de Castro Faria, B. Farizon-Mazuy and M.J. Gaillard, *J. Phys.: Condensed Matter* **5**, A275 (1993).
 42. F.J. Rogers, H.C. Graboske Jr. and D.J. Harwood, *Phys. Rev. A* **1**, 1537 (1970).
 43. L.H. Toburen, M.Y. Nakai and R.A. Langley, *Phys. Rev.* **171**, 114 (1968).
 44. H. Rothard, J.P. Thomas, J. Remillieux, J.C. Poizat, R. Kirsch, K.O. Groeneveld, M. Fallavier and D. Dauvergne, in *Ionization of Solids by Heavy Particles*, ed. by R.A. Baragiola, Plenum, New York, 215 (1993).
 45. K. Kroneberger, A. Clouvas, G. Schlusser, P. Koschar, J. Kemmler, H. Rothard, C. Biedermann, O. Heil, M. Burkhard and K.O. Groeneveld, *Nucl. Instr. Meth. Phys. Res. B* **29**, 621 (1988).
 46. W. Meckbach, G. Braunstein and N. Arista, *J. Phys. B* **8**, L344 (1975).
 47. D.P. Almeida, N.V. de Castro Faria, F.L. Freire Jr., R. Kirsch and A.G. de Pinho, *Phys. Rev. B* **37**, 7182 (1988).
 48. B. Svensson and G. Holmen, *Phys. Rev. B* **25**, 3056 (1982).
 49. T.A. Tombrello, *Nucl. Instr. Meth. Phys. Res. B* **99**, 225 (1995).
 50. W.L. Brown and M. Sosnowski, *Nucl. Instr. Meth. Phys. Res. B* **102**, 305 (1995).
 51. K. Boussofiane-Baudin, A. Brunelle, P. Chaurand, S. Della-Negra, J. Depaw, P. Håkansson and Y. Le Beyec, *Nucl. Instr. Meth. Phys. Res. B* **88**, 61 (1994); S. Della-Negra, IPN-Orsay Les Infos n. 109, sept. 1995.